ISSN: 0975-8585

Research Journal of Pharmaceutical, Biological and Chemical Sciences

Formation of the layer composition for a solid-state quantum dot sensitized solar cell ZnO|SnS|CuSCN.

V.V. Ivanov[1]*, G.V. Tsepilov[1], I.V. Enyutin[2], and S.M.-K. Bakmaev[1].

[1]CJSC "TECHNOCOMPLEKT", 10a Shkol'naya st., Dubna, Moscow oblast, 141981 Russia.
[2]OOO "TURBOENERGOREMONT", premises 170N, block A, 114 Leninskii prospect, Saint Petersburg, Leningradskaya oblast, 198207, Russia.

ABSTRACT

For the purpose of the development of a new design of a solid-state quantum dot sensitized solar cell (SS-QDSSC), pulse electrodeposition of 1-D ZnO arrays was performed, as well as deposition of SnS quantum dots and thin film of p-CuSCN wide band gap semiconductor using the Successive Ionic Layer Adsorption and Reaction (SILAR) method. The paper studies the morphology, structure and optical properties of all semiconductor layers. The diode characteristic of the SS-QDSSC with a new design developed by our team is demonstrated, confirming its functionality.

Keywords:solid-state hybrid solar cell, one-dimensional ZnO structure, SnS quantum dots, pulse electrodeposition, successive ionic layer adsorption and reaction.

Corresponding author

ISSN: 0975-8585

INTRODUCTION

The increase in the worldwide demand for inexpensive renewable energy sources motivates researchers to develop new approaches to solar energy applications. Photovoltaic conversion by using solar cells (SC) is a clean technology for electric power production. Nevertheless, high costs related to the production of widely used silicon wafers based SCs at the stages of materials synthesis and further production of devices decrease the economic efficiency of the wide application of silicon solar batteries. Solid-state quantum dot sensitized solar cells (SS-QDSSCs) based on the nanostructures of wide band gap electronic semiconductors with a large surface area where photosensitive semiconductor quantum dots (QD) are deposited with a layer of p-type wide band gap semiconductor deposited above them are considered to be perspective inexpensive and effective SCs [1-3]. This solar cell concept allows to use semiconductor materials of a relatively low structural quality due to the low distance that a photogenerated carrier should overcome before it comes into semiconductor phases of corresponding type which are designated for electrons and holes transportation. The low cost of SS-QDSSC is not only based on the application of inexpensive materials but also on the possibility of cheap production processes usage applicable for wide production of these SCs. Unlike currently classical electrochemical solar cells sensitized by dyes (DSSC) or by quantum dots (QDSSC), the SS-QDSSCs are considered to be a renewed version of this old concept [4] and do not contain liquid or gelatinous electrolyte that certainly brings advantages of usage. Presently being developed fully solid-state SS-QDSSCs have a nanostructural semitransparent layer made of wide band gap n-type semiconductor, for example, mesoporous TiO_2 or one-dimensional (1-D) ZnO array or hierarchical ZnO nanostructures, which is covered by ultra-thin layer of light absorbing semiconductor quantum dots. Then a thin film of wide band gap p-type semiconductor is deposited onto QD layer. In the majority of up-to-date designs of quantum dot sensitized solar cells of various types the toxic materials for QD were used, such as CdS, CdSe, CdTe and PbS [2-5]. It was suggested [6] to use at the surface of porous TiO_2 layer the quantum dots that are made of tin sulfide (SnS) which is not only nontoxic but also widespread in nature. However, a quite complex two-stage Sol-Gel technology that includes two annealings was used at [6] for TiO_2 deposition onto glass substrate with a transparent electroconductive layer made of fluorine doped tin oxide (FTO). Our team study offers for SS-QDSSC design the nanostructured 1-D ZnO array to be utilized as the wide band gap n-type semiconductor with SnS quantum dots deposited on it, which is to be grown directly at FTO surface by means of inexpensive single-stage pulse electrolysis method suitable for large-scale production. Its advantages are described at [9-10]. For the deposition of SnS quantum dots and further deposition of a thin film of wide band gap p-CuSCN semiconductor above them the inexpensive and available Successive Ionic Layer Adsorption and Reaction (SILAR) method was used, which received a wide recognition among manufacturers of similar solar cells [1-4, 6-8]. The present work studies the morphology, structure and optical properties of components and demonstrates the diode characteristic of SS-QDSSC with a new design developed by our team.

EXPERIMENTAL TECHNIQUE

Obtaining of zinc oxide nanorods is performed similar to [10-12] by pulse cathode electrochemical deposition at the temperature-controlled three-electrode electrochemical cell with unmixed water electrolyte containing 0.01 M $Zn(NO_3)_2$ and 0.1 M $NaNO_3$ at 70 °C. For the substrates (cathodes or main electrodes) the FTO wafers model TEC 7 made by company Pilkington, USA were used. A platinum coil was used for counter electrode, and saturated silver chloride electrode Ag/AgCl was for reference electrode. According to the recommendation [9], at the first stage of electrodeposition a nucleating ZnO layer was obtained by suppling a constant voltage U = -1.3 V to FTO electrode in the same electrolyte during 30 seconds. After that for pulse electrolysis rectangular pulses of voltage were supplied to cathode substrate during 30 minutes by means of pulse potentiostat PI-50-1.1 equipped with programmer PR-8. Lower cathode voltage limit U_{off} was equal to -0.7 V, upper limit was equal to $-U_{on}$ = -1.3 V (the voltage is given relatively to the reference electrode Ag/AgCl). A duty cycle, i.e. the relation of the pulse width to the sum of pulse and pause width, and a frequency as a reciprocal of sum of pulse and pause width were 0.4 and 2 Hz accordingly. In this way ZnO nanorods arrays of around 1.5 µm width shown in Figure 1 were obtained.

ISSN: 0975-8585

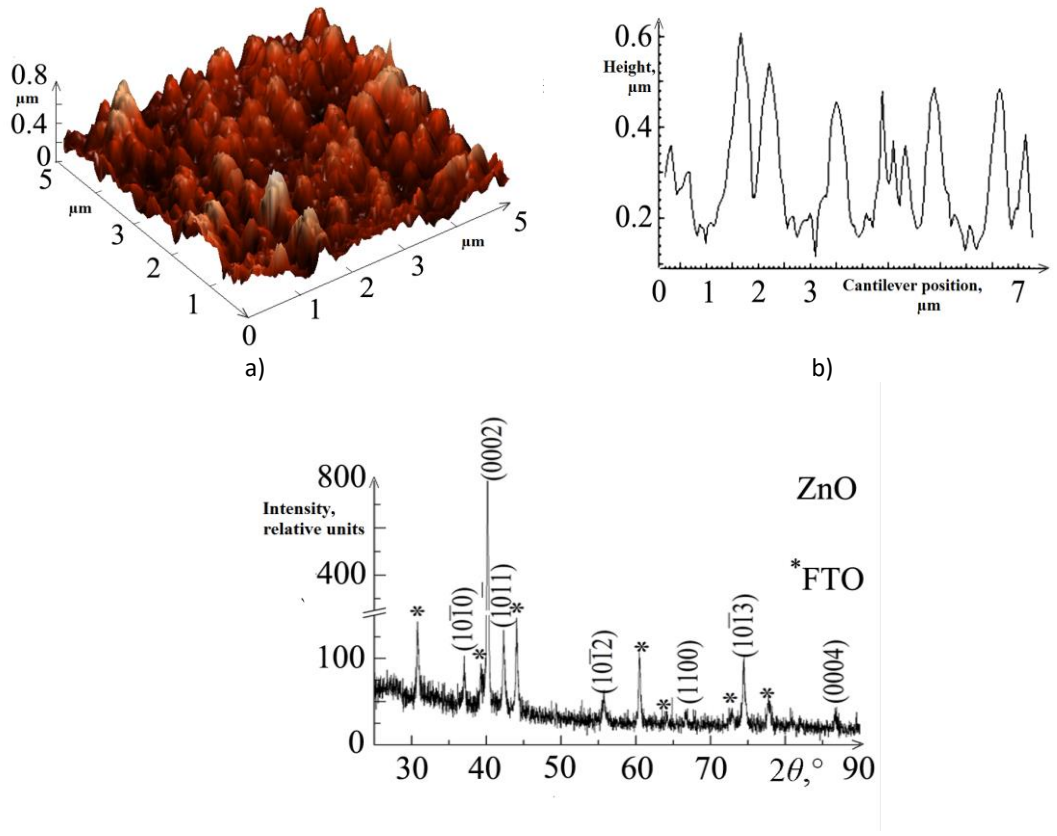

Figure 1. A 3D image of ZnO achieved by AFM (a) and corresponding zinc oxide nanorods profile (b). X-ray ZnO defectogram (c).

For making tin sulfide quantum dots layers by SILAR method the K8 glass substrate or FTO wafer with ZnO nanorods array were successively submerged in aqueous solution of 0.01 M $SnSO_4$ (during 20 seconds at 70-80 °C), then in distilled water (during 10 seconds at 20 °C), then in aqueous solution of Na_2S 0.01 M (during 20 seconds at 20 °C) and again in distilled water (during 10 seconds at 20 °C). This procedure is one cycle of SILAR (*n* = 1). For making tin sulfide quantum dots with variable dimensions and optical properties the cycle number for SnS QD production varied from *n* = 20 to *n* = 140.

CuSCN layers depositions onto glass substrates and onto layer composition surface of glass|FTO|ZnO|SnS by SILAR method were performed according to the recipe offered in [8]. For cationic precursor the aqueous solution of 0.1 M $CuSO_4$ and 0.1 M $Na_2S_2O_3$ was used where a copper thiosulfate complex was formed. The substrate was submerged in cationic precursor for 10 seconds. A monolayer of copper ions Cu^+ was absorbed on the substrate surface, and non-absorbed ions were removed by washing the substrate in distilled water during 5 seconds. For the reaction with SCN ions the substrate was submerged in anionic precursor 0.00625 M KSCN during 20 seconds. The particles and ions that were loosely bound with the substrate were removed by distilled water during 5 seconds. The above-said procedures make up one CuSCN SILAR cycle. CuSCN SILAR cycles were repeated 52 times (*n* = 52). In this way a copper thiocyanate film on K8 glass substrate was produced for the research of the optical properties and structure of CuSCN, as well as SS-QDSSC base was produced in a form of layer composition of glass|FTO|ZnO|SnS.

The upper electric contact was achieved by the pressure of wafer glass|FTO to the copper thiocyanate film surface in the way described in [13]. Figure 2a outlines a design of the produced layer composition of glass|FTO|ZnO|SnS|CuSCN|FTO|glass for solid-state hybrid solar cell with SnS quantum dots.

ISSN: 0975-8585

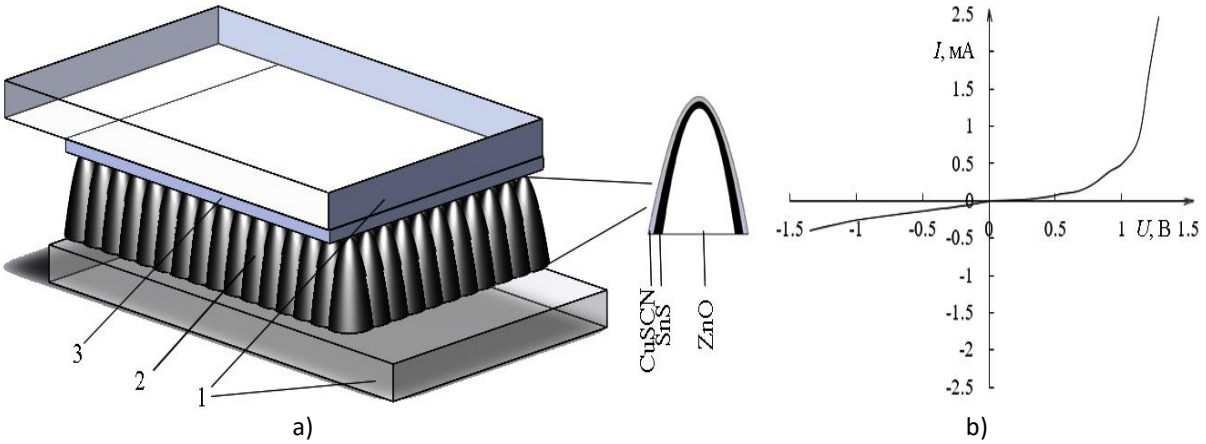

Figure 2. A layout of layer composition of glass|FTO|ZnO|SnS|CuSCN|FTO|glass for solid-state hybrid solar cell with SnS quantum dots (a). A dark volt-ampere characteristic of experimental sample of SS-QDSSC (b).

The study of the optical properties of nanostructured zinc oxide layers, SnS quantum dots and CuSCN thin films was performed by spectrophotometer CF-2000. For check samples upon optical transmission spectra $T(\lambda)$ registration corresponding substrates were used (glass|FTO for ZnO and K8 glass for SnS and CuSCN). The absorption spectra (for optical density) $A(\lambda)$ were obtained from the relationship $A = -\lg T$. Forbidden band width for optical transitions E_g for ZnO layers and SnS QD was determined similar to [12] by means of extrapolation of linear section of relationship between $[-\ln(T)\cdot h\nu]^2$ and $h\nu$ to energies axis. Thickness d of CuSCN films was defined by interference peaks:

$$d = \frac{M\lambda_1\lambda_2}{2(n(\lambda_1)\lambda_2 - n(\lambda_2)\lambda_1)}, \qquad (1)$$

where M – the number of maximums between λ_1 and λ_2, λ_1 and λ_2 – wavelengths, corresponding to the maximums at $T(\lambda)$ spectrum, n – refractive index of CuSCN, corresponding to the wavelengths λ_1 and λ_2.

Forbidden band width determination for direct optical transitions of CuSCN films was performed in accordance with [8], i.e. the data about optical absorption coefficient $\alpha = -d^{-1}\cdot\ln(T)$ was used as well as extrapolation of linear section of relationship between $(\alpha\cdot h\nu)^2$ and $h\nu$ to energies axis. To determine forbidden band width for indirect allowed optical transitions the relationship between $(\alpha\cdot h\nu)^{1/2}$ and $h\nu$ was used similarly. The scattering factor (Hf) was calculated in accordance with [12] as a ratio of radiosity to overall radiosity R (the amount of radiosity and specular reflection).

For the purpose of the analysis of the structure and substructure parameters of ZnO arrays, SnS quantum dots layers and thin CuSCN films the X-ray spectra (XRD) was registered by DRON-4 diffractometer in CoK_α ($\lambda_{CoK\alpha}$ = 1.7889 Å) emission. Scanning was performed in Bragg-Brentano focusing (ϑ–2ϑ). The processing of the obtained X-ray diffractograms (background removal, $K_{\alpha1}$ – $K_{\alpha2}$ doublet separation, etc.), as well as the calculations of diffraction lines profile parameters were performed by using New_Profile v.3.4 (486) and OriginPro v.7.5 software. The existence of crystal phases was disclosed by the comparison of experimental X-ray diffractograms data with JCPDSs reference database using PCPDFWIN v.1.30 software. Coherent scattering regions (CSR) estimation was performed by the analysis of X-ray diffraction maximums broadening according to Williamson–Hall approach [14] and according to Sherrer method [15] taking into consideration the existence of instrumental broadening.

For electrodeposited zinc oxide arrays texture analysis as per Harris method the values for integrated intensity of X-ray diffractometer peaks were used in accordance with [16]. For each peak a polar density $P(hkl)$ was calculated which defines the probability of coincidence of normal to crystal surface with normal to (hkl) plane, in other words, which defines a quantity of crystallites with (hkl) plane parallel to image surface. Polar densities were calculated for all registered X-ray diffractometer peaks, values of $P(hkl) >> 1$ were assign to texture axes.

ISSN: 0975-8585

The morphology research of zinc oxide array surface was performed by semi-contact atomic force microscopy (AFM) method on Nano Laboratory Ntegra Prima NT-MDT atomic microscope.

For polarity of conductivity determination the standard thermoprobe method [17] was used. The measurements of dark volt-ampere characteristics for layer composition glass|FTO|ZnO|SnS|CuSCN|FTO| glass were performed according to characteristic tracer scheme [18] using industrial characteristic tracer L2-56 with direct visualization of volt-ampere characteristic on the monitor.

RESULTS DISCUSSION

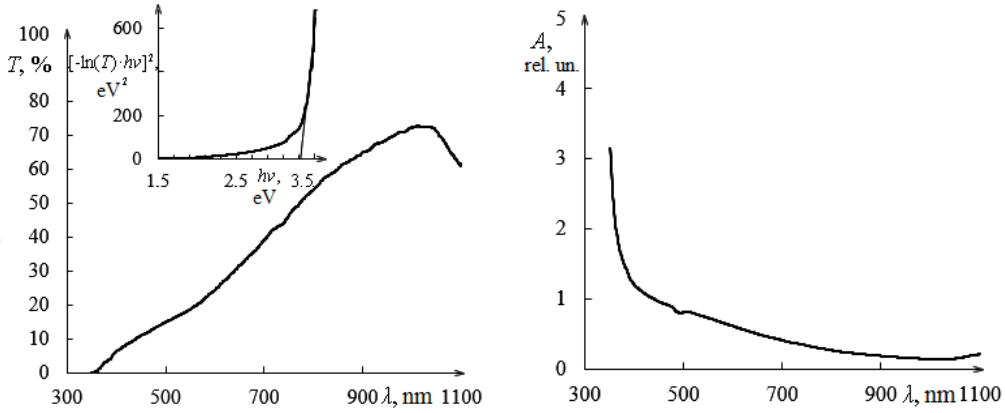

Figure 3. Optical properties of nanostructured ZnO array: optical transmission spectrum (a), diagram for Eg estimation (in the insertion), optical absorption spectrum (b).

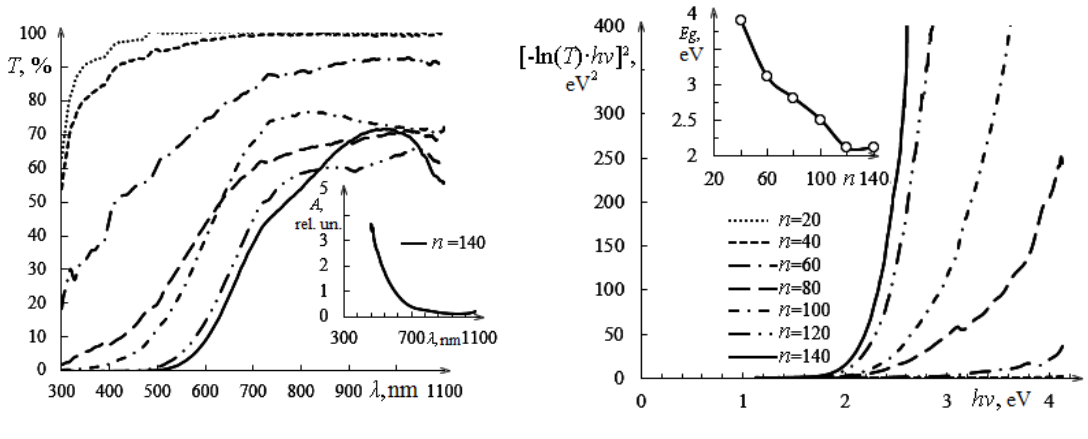

Figure 4. Optical properties of SnS quantum dots layers deposited onto glass substrates by SILAR method at *n* number of cycles: optical transmission spectrum (a), optical absorption spectrum of SnS quantum dots layer obtained by SILAR at *n* = 140 (in the insertion); diagram for Eg estimation of SnS (b), relationship between E_g and *n* (in the insertion).

Figures 1a and 1b show obtained by AFM 3D images of surface and surface profile of pulse electrodeposited ZnO layer that demonstrate that the layer appears to be the nanorods arrays located perpendicular to substrate surface. X-Ray diffractogram analysis in Figure 1c shows that ZnO array is monophase and has hexagonal ZnO structure of wurtzite modification (JCPDS PDF No. 361451). Electrodeposited zinc oxide array is nanocrystal with coherent scattering range from 70 to 190 nanometers; it is characterized by increased crystal lattice parameters along *c* axis (*c* = 5.22 Å) compared to reference ZnO (as per JCPDS PDF No. 361451, where *c* = 5.207 Å), also it is characterized by insufficient microstress ~ 10^{-3} and by residual compression stress of ~ -0.4 GPa. ZnO array has an axial structure P(002) = 2.35, and therefore has a

preferred directional orientation <001>, that is perpendicular to substrate surface which is concordant to the AFM data.

Optical properties pulse electrodeposited nanostructured ZnO array (Figure 3) show its sufficient transparency and small absorption at visible spectral region. Forbidden band width for direct optical transmission is equal to 3.36 eV, that is almost equal to E_g = 3.37 eV for monocrystal ZnO. Measurements according to thermoprobe method show that pulse electrodeposited zinc oxide has typical for ZnO n-type conductivity.

Figure 4 shows the results of the research of optical properties of SnS quantum dots layers deposited at glass surfaces. As seen in Figure 4a, with the increase of SILAR cycles not only the visible light transmission of SnS layers decreases, but also an absorption band shifts into long-wave region.

At the box of Figure 4a an intensive light absorption by SnS layer obtained by SILAR at n = 140 is highlighted, almost at all visible spectrum, and Figure 5a shows this layer photo. Figure 5b demonstrates the X-ray diffractogram of the same specimen of Herzenbergite modification (Herzenbergite, β-SnS, JCPDS PDF No. 390354) where there are three weak SnS peaks (120), (101) and (111).

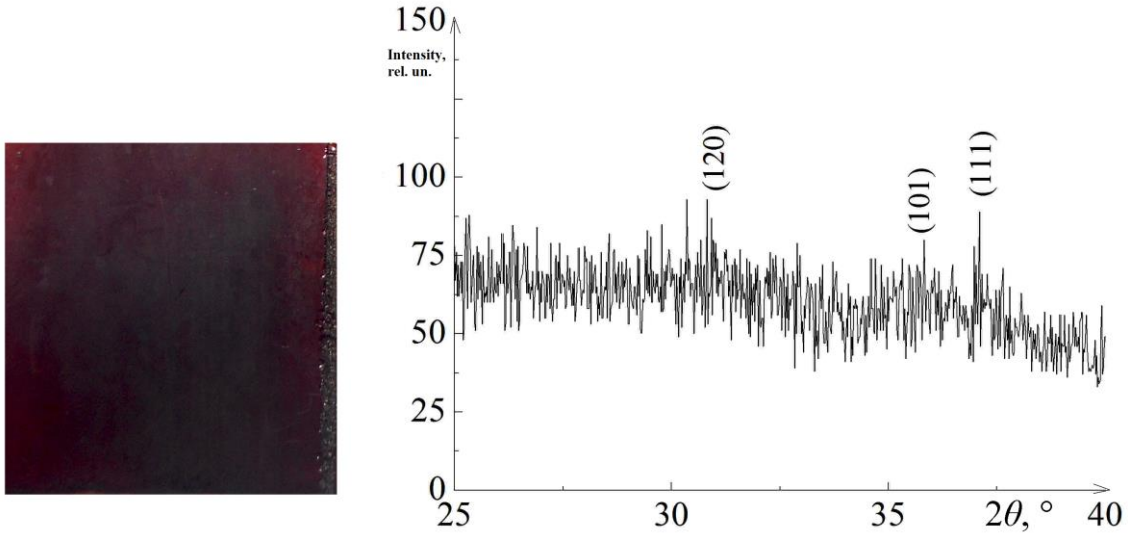

a) b)

Figure 5. Picture of the glass wafer with visible light absorbing SnS layer, obtained by SILAR n = 140 (a) and its X-ray diffractogram (b). Diffraction peaks are related to SnS Herzenbergite modification (Herzenbergite, β-SnS, JCPDS PDF No. 390354).

So far as dimensions of SnS particles monotonically increasing with the increase in the number of cycles in accordance with [6], the obtained SnS nanoparticles at maximal n = 140 were of the biggest size. Following the calculations according to Sherrer method, their coherent-scattering region was ~ 28 nanometers. It should be noted that X-ray diffractograms of SnS layers obtained at less SILAR cycles number does not have peaks, which, in our opinion, is an evidence of layers X-ray amorphism caused by smaller dimensions of SnS nanoparticles. Experimental results obtained by our team are well consistent with those in literature. For example, a comparative analysis of the data from electronic transmission microscopy and X-ray diffractometry carried out in [20] showed that only for SnS QD bigger than 10-14 nanometers two weak peaks (120) and (111) were registered at X-ray diffractograms.

Figure 4b demonstrates the characteristic effect of forbidden band width E_g decrease with increase of n, and therefore with increase of SnS nanoparticles. By increasing SILAR cycles from n = 20 to n = 140 the E_g of tin sulfide was reduced from 3.9 to 2.1 eV. According to [6], the rated value of Bohr radius SnS is 7.24 nanometers, that is to say strictly, the quantum dots are the nanoparticles of tin sulfide, the dimensions of which are less than this value. Since the range for forbidden band width for SnS given in literature very large and is between 1.0 to 2.3 eV [19], it is difficult to determine the required number of SILAR cycles that provide a

ISSN: 0975-8585

removal of quantum-dimensional effect at SnS nanoparticles due to their excess of Bohr radius. But taking into account the relationship character between E_g and n in Figure 4b, $n \geq 120$. Assuming that the design of solid state hybrid quantum dots solar cell requires extremely thin QD layer on the one hand and the maximum absorption of the light by SnS nanoparticles on the other hand, the SnS absorbing QD layer deposited at n = 100 SILAR cycles was used as a compromise option for SS-QDSSC production in our case. Above this layer for obtaining a wide band gap holes semiconductor material the copper thiocyanate film was deposited by 52 SILAR cycles.

Figure 6 demonstrates the optical properties of similar CuSCN film deposited on check specimen made of K8 glass. The film width according to the calculation of equation (1) was ~ 0.6 μm (n = 1.85 according to [21]). As shown in Figure 6a, the film of copper thiocyanate is transparent in all visible range and has forbidden band width for direct and indirect optical transmissions of 3.9 eV and 3.5 eV which are characteristic for CuSCN [8; 22–23]. Figure 6b shows that interference oscillations are not only likely for transmission spectrum but also for CuSCN film diffraction spectrum. However, resulting from a light scattering factor diagram (the insertion in Figure 6b), it was not absolutely even and perfectly transparent. Figure 6b shows X-ray diffractogram of this film confirming that it is a hexagonal modification of CuSCN with wurtzite structure (Wurtzite *β*-CuSCN PDF No. 290581).

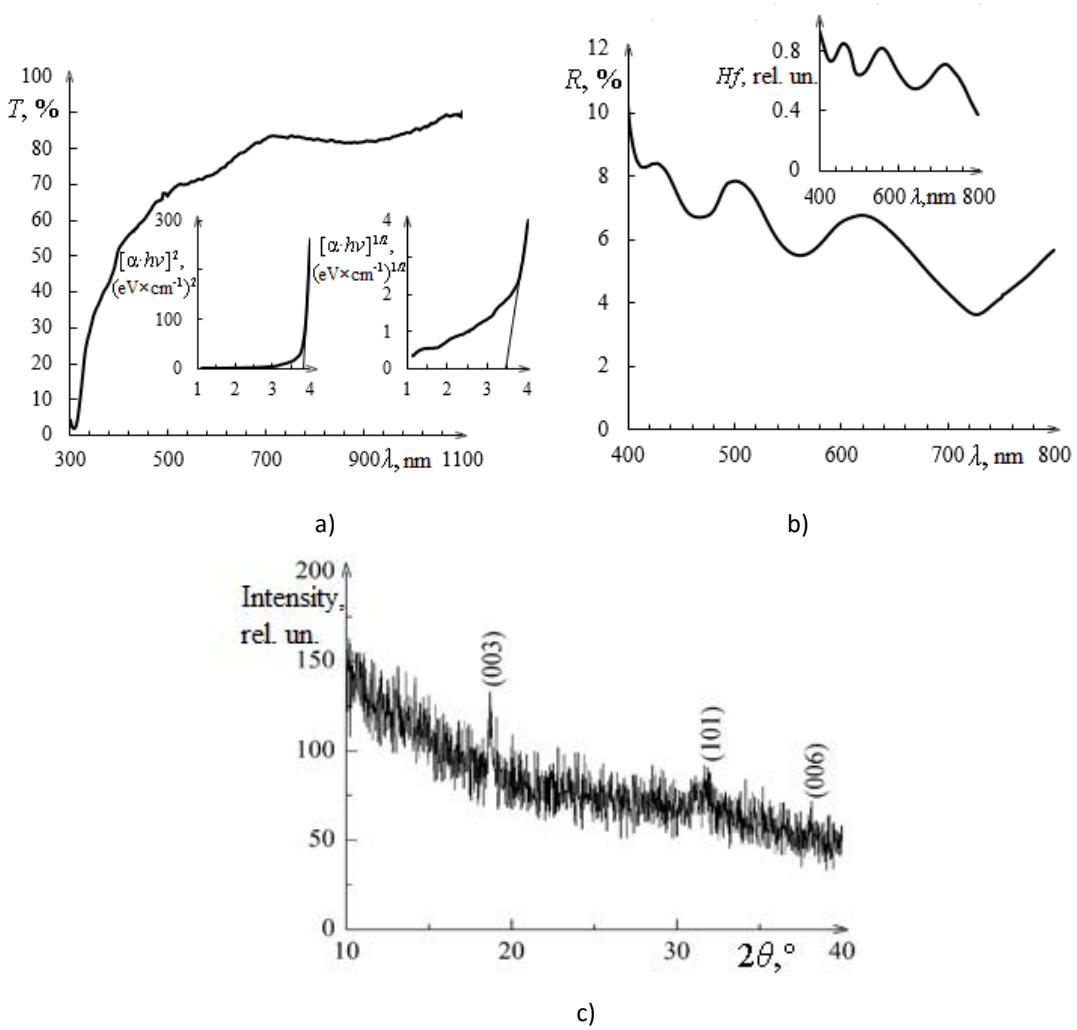

Figure 6. Optical properties and crystal structure of CuSCN film of ~0.6 μm width deposited at K8 glass: optical transmission spectrum (a), diagram for forbidden band width for direct and indirect optical transmissions (in the nsertion); optical reflex spectrum (b), diagram of relation between scattering factor and wavelength (in the insertion); X-ray diffractogram (c). Diffraction peaks are related to CuSCN wurtzite modification (Wurtzite β-CuSCN PDF No. 290581).

Calculations according to Williamson–Hall approach show that the dimensions of coherent-scattering regions of this film are within 40-70 nanometers, microstresses are from $2 \cdot 10^{-3}$ to $4 \cdot 10^{-3}$. Measurements by

thermoprobe method show that the copper thiocyanate film obtained by SILAR method has p-type conductivity which is characteristic for CuSCN.

Produced layer composition glass|FTO|ZnO|SnS|CuSCN was covered above by glass|FTO waffer. Volt-ampere characteristic of solid-state hybrid solar cell which is produced by this way is shown in Figure 2b. It demonstrates the existence of rectifying barrier which is conditioned by a presence of conjugation zone where integrated electric field of *p-i-n* heterojunction is concentrated, which is characteristic for SS-QDSSC.

The analysis of the form of the reverse-bias region of the volt-ampere characteristic by using its tangent allowed to calculate a shunt resistance for layer composition glass|FTO|ZnO|SnS|CuSCN|FTO|glass which appeared to be equal to 5 kilohms, i.e. providing a functionality for SS-QDSSC of a new design.

Semiconductor materials ZnO and TiO_2 have very similar zone structures by E_g value and by band edges locations. However, for production of nanostructured zinc oxide arrays there are more possibilities, for example, 1-D ZnO can be obtained by inexpensive and available pulse electrodeposition method, as shown in the present work. Furthermore, this method can be applied for large surfaces. As it was demonstrated by our team, the other two functional layers of solid state hybrid solar cell which consist of QD SnS and CuSCN thin film are also successfully produced by well controlled, simple, cheap and available SILAR method. None of any toxic, volatile or fire-hazardous reagents were utilized by our team in any of these methods. For production of layer composition for offered new SS-QDSSC design expensive and power-consuming vacuum equipment was not applied as well as any annealings were not utilized. Nevertheless, we managed to create a functional *p-i-n* heterojunction which is the basis of this hybrid solar cell.

SUMMARY

Our team demonstrates in this work the formation of the layer composition of a solid-state hybrid solar cell ZnO|SnS|CuSCN with two FTO contacts. The electrochemical and chemical methods to produce it are safe for the environment, inexpensive and suitable for high volume production. The results of the research of the structure and optical properties of separate layers and the volt-ampere characteristic of the complete layer composition confirm the potential of a SS-QDSSC designed by our team as a cheap and effective alternative for the existing designs of solar cells.

ACKNOWLEDGEMENTS

This article is prepared within the framework of applied scientific research and experimental developments (ASRED) according to the Subsidy Agreement No. 14.579.21.0113 dated October 27, 2015, with the financial support of The Ministry of Education and Science of the Russian Federation. Unique identifier PNIER RFMEFI57915X0113.

REFERENCES

[1] Babu V.J., Vempati S., Sundarrajan S., Sireesha M., Ramakrishna S. Effective nanostructured morphologies for efficient hybrid solar cells. Solar Energy. 2014. V. 106. P. 1-22.

[2] Nikhil A., Thomas D.A., Amulya S., Mohan S.R., Kumaresan D. Synthesis, characterization, and comparative study of CdSe–TiO_2 nanowires and CdSe-TiO_2 nanoparticles. Solar Energy. 2014. V. 106. P. 109-117.

[3] Li Y., Wei L., Chen X., Zhang R., Sui X., Chen Y., Jiao J., Mei L. Efficient PbS/CdS co-sensitized solar cells based on TiO_2 nanorod arrays. Nanoscale Research Letters. 2013. V. 8:67. P. 1-9.

[4] Lee H.J., Leventis H.C., Moon S.-J., Chen P., Ito S., Haque S.A., Torres T., Nüesch F., Geiger T., Zakeeruddin S.M., Grätzel M., Nazeeruddin M.K. PbS and CdS Quantum Dot-Sensitized Solid-State Solar Cells: “Old Concepts, New Results”. Advanced Functional Materials. 2009. V. 19, No. 17. P. 2735-2742.

[5] Khrypunov G., Klochko N., Volkova N., Lyubov V., Li T. Single-phase cadmium telluride thin films deposited by electroless electrodeposition. Japanese Journal of Applied Physics. 2011. V. 50, No. 17. P. 05FH04-1–05FH04-2.

[6] Deepa K.G, Nagaraju J. Development of SnS quantum dot solar cells by SILAR method. Materials Science in Semiconductor Processing. 2014. V. 27. P. 649-653.

[7] Lindroos S., Puišo J., Tamulevičius S., Leskelä M. CdS-PbS Multilayer Thin Films Grown by the SILAR Method. Solid State Phenomena. 2014. V. 99-100. P. 243-246.
[8] Sankapal B.R., Goncalves E., Ennaoui A., Lux-Steiner M.Ch. Wide band gap p-type windows by CBD and SILAR methods. Thin Solid Films. 2004. V. 451-452. P. 128-132.
[9] Skompska M., Zarębska K. Electrodeposition of ZnO nanorod arrays on transparent conducting substrates–a review. Electrochimica Acta. 2014. V. 127. P. 467-488.
[10] Klochko N.P., Khrypunov G.S., Myagchenko Y.O., Melnychuk E.E., Kopach V.R., Klepikova E.S., Lyubov V.M., Kopach A.V. Controlled growth of one-dimensional zinc oxide nanostructures in the pulsed electrodeposition mode. Semiconductors. 2012. V. 46. P. 825-831.
[11] Klochko N.P., Klepikova K.S., Tyukhov I.I., Myagchenko Y.O., Melnychuk E.E., Kopach V.R., Khrypunov G.S., Lyubov V.M., Kopach A.V. Structure and optical properties of sequentially electrodeposited ZnO/Se bases for ETA solar cells. Solar Energy. 2015. V. 120. P. 330-336.
[12] Klochko N.P., Klepikova E.S., Khrypunov G.S., Volkova N.D., Kopach V.R., Lyubov V.N., Kirichenko M.V., Kopach A.V. Antireflective nanostructured zinc oxide arrays obtained by pulse electrodeposition. Semiconductors physics and technique 2015. V. 49. P. 219-229
[13] Chao X., Lei C., Hongchun Y. Study on the synthesis, characterization of p-CuSCN/n-Si heterojunction. The Open Materials Science Journal. 2013. V. 7. P. 29-32.
[14] Tsybulia S.V. Introduction to nanocrystals structural analysis. Novosibirsk State University. Novosibirsk. 1980.
[15] Kuzmicheva G.M. Radiography of nanoscale objects.Part I.. Tutorial. M. V. Lomonosov Moscow State Institute of Fine Chemical Technology. Moscow. 2010.
[16] Structure and physical properties of solid body. Laboratory practical work. Edited by Palatnik L.S. Kiev. High School. 1983.
[17] Axelevitch A., Golan G. Hot-probe method for evaluation of majority charged carriers concentration in semiconductor thin films. Facta Universitatis Series: Electronics and Energetics, 2013.
[18] Mazda F.F. Electronic Instruments and Measurement Techniques. Cambridge: Cambridge University Press, 1987.
[19] Shaposhnikov V.L., Krivosheeva A.V., Borisenko V.E., Lazzari J.-L. Structure, electronic and optical properties of tin sulfide. ScienceJet. 2012. V. 1: 16. P. 1-4.
[20] Deepa K.G., Nagaraju J. Growth and photovoltaic performance of SnS quantum dots. Materials Science and Engineering B. 2012. V. 177. P 1023-1028.
[21] Pattanasattayavong P., Ndjawa G.O.N., Zhao K., Chou K.W., Yaacobi-Gross N., O'Regan B.C., Amassian A., Anthopoulos T.D. Electric field-induced hole transport in copper(I) thiocyanate (CuSCN) films processed from solution at room temperature. Chemical Communications. 2013. V. 49. P. 4154-4156.
[22] Perumal A., Faber H., Yaacobi-Gross N., Pattanasattayavong P., Burgess C., Jha S., McLachlan M.A., Stavrinou P.N., Anthopoulos T.D., Bradley D.D.C. High-Efficiency, Solution-Processed, Multilayer Phosphorescent Organic Light-Emitting Diodes with a Copper Thiocyanate Hole-Injection/Hole-Transport Layer. Advanced Materials. 2015. V. 27. P. 93-100.
[23] Zhao K., Munir R., Yan B., Yang Y., Kim T., Amassian A. Solution-processed inorganic copper (I) thiocyanate (CuSCN) hole transporting layers for efficient p-i-n perovskite solar cells. Journal of Materials Chemistry A. 2015. V. 3. P. 20554-20559.